

Proof-of-principle demonstration of a pilot bunch comagnetometer in a stored beam

J. Slim^{1,*}, F. Rathmann^{2,†,‡}, A. Andres^{1,2}, V. Hejny², A. Nass², A. Kacharava², P. Lenisa³, N. N. Nikolaev^{4,§}, J. Pretz^{1,2}, A. Saleev^{3,||}, V. Shmakova^{3,¶}, H. Soltner⁵, F. Abusaif^{1,2,**}, A. Aggarwal⁶, A. Aksentev⁷, B. Alberdi^{1,2,††}, L. Barion³, I. Bekman^{2,‡‡}, M. Beyß^{1,2}, C. Böhme², B. Breitkreutz^{2,§§}, N. Canale³, G. Ciullo³, S. Dymov³, N.-O. Fröhlich^{2,*}, R. Gebel², M. Gaisser¹, K. Grigoryev^{2,§§}, D. Grzonka², J. Hetzel², O. Javakhishvili⁸, V. Kamerdzhiiev^{2,§§}, S. Karanth^{6,|||}, I. Keshelashvili^{2,§§}, A. Kononov³, K. Laihem^{1,§§}, A. Lehrach^{1,2}, N. Lomidze⁹, B. Lorentz¹⁰, G. Macharashvili⁹, A. Magiera⁶, D. Mchedlishvili⁹, A. Melnikov⁷, F. Müller^{1,2}, A. Pesce², V. Poncza², D. Prasuhn², D. Shergelashvili⁹, N. Shurkhno^{2,§§}, S. Siddique^{1,2,§§}, A. Silenko¹¹, R. Stassen², E. J. Stephenson¹², H. Ströher², M. Tabidze⁹, G. Tagliente¹³, Y. Valdau^{2,§§}, M. Vitz^{1,2}, T. Wagner^{1,2,§§}, A. Wirzba¹⁴, A. Wrońska⁶, P. Wüstner¹⁵ and M. Žurek^{2,¶¶}

(JEDI Collaboration)

¹III. Physikalisches Institut B, RWTH Aachen University, 52056 Aachen, Germany

²Institut für Kernphysik, *Forschungszentrum Jülich*, 52425 Jülich, Germany

³University of Ferrara and Istituto Nazionale di Fisica Nucleare, 44100 Ferrara, Italy

⁴L.D. Landau Institute for Theoretical Physics, 142432 Chernogolovka, Russia

⁵Institute of Technology and Engineering, *Forschungszentrum Jülich*, 52425 Jülich, Germany

⁶Marian Smoluchowski Institute of Physics, Jagiellonian University, 30348 Cracow, Poland

⁷Institute for Nuclear Research, Russian Academy of Sciences, 117312 Moscow, Russia

⁸Department of Electrical and Computer Engineering, Agricultural University of Georgia, 0159 Tbilisi, Georgia

⁹High Energy Physics Institute, Tbilisi State University, 0186 Tbilisi, Georgia

¹⁰GSI Helmholtzzentrum für Schwerionenforschung, 64291 Darmstadt, Germany

¹¹Bogoliubov Laboratory of Theoretical Physics, Joint Institute for Nuclear Research, 141980 Dubna, Russia

¹²Indiana University, Department of Physics, Bloomington, Indiana 47405, USA

¹³Istituto Nazionale di Fisica Nucleare sez. Bari, 70125 Bari, Italy

¹⁴Institute for Advanced Simulation, *Forschungszentrum Jülich*, 52425 Jülich, Germany

¹⁵Zentralinstitut für Engineering, Elektronik und Analytik, *Forschungszentrum Jülich*, 52425 Jülich, Germany



(Received 17 October 2023; accepted 11 March 2025; published 13 June 2025)

In polarization experiments at storage rings, one of the challenges is to maintain the spin-resonance condition of a radio-frequency spin rotator with the spin precessions of the orbiting particles. Time-dependent variations of the magnetic fields of ring elements lead to unwanted variations of the spin-precession frequency. We report here on a solution to this problem by shielding (or masking) one of the bunches stored in the ring from the high-frequency fields of the spin rotator, so that the masked pilot bunch acts as a comagnetometer for the other signal bunch, tracking fluctuations in the ring on a time scale of about one second. While the new method was developed primarily for searches of electric dipole moments of charged particles, it may have far-reaching implications for future spin physics facilities, such as the EIC and NICA.

DOI: [10.1103/PhysRevResearch.7.023257](https://doi.org/10.1103/PhysRevResearch.7.023257)

*Present address: Deutsches Elektronen-Synchrotron, 22607 Hamburg, Germany.

†Present address: Brookhaven National Laboratory, Upton, New York 11973, USA.

‡Contact author: frathmann@bnl.gov

§Present address: N.N. Bogoliubov Laboratory of Theoretical Physics, 141980 Dubna, Russia.

||Present address: Institute for a Sustainable Hydrogen Economy, Forschungszentrum Jülich, 52428 Jülich, Germany.

¶Present address: Brookhaven National Laboratory, Upton, New York 11973, USA.

**Present address: Karlsruhe Institute of Technology, 76344 Eggenstein-Leopoldshafen, Germany.

††Present address: Humboldt-Universität zu Berlin, Institut für Physik, 12489 Berlin, Germany.

‡‡Present address: Institute of Technology and Engineering, Forschungszentrum Jülich, Jülich, Germany.

§§Present address: GSI Helmholtz Centre for Heavy Ion Research, 64291 Darmstadt, Germany.

|||Present address: H. Niewodniczański Institute of Nuclear Physics, Polish Academy of Sciences, 31-342, Kraków, Poland.

¶¶Present address: Argonne National Laboratory, Lemont, Illinois 60439, USA.

I. INTRODUCTION

Controlled rf-driven spin rotations, in particular the spin flip (SF), are indispensable for nuclear physics experiments with polarized particles (see, e.g., Refs. [1,2], for reviews, see Refs. [3,4]). Extensive spin physics experiments in storage rings are either performed [5–9] or prepared, in particular to search for physics beyond the standard model (BSM) [9–20]. For a precise measurement of the spin-flip frequency, it is important to maintain the exact spin resonance condition over a long period of time to allow a large number of spin flips during the continuous operation of an rf spin rotator.

In precision experiments, the instability of magnetic fields has to be mitigated by comagnetometers, which continuously gauge magnetic fields independently. For example, in the search for the electric dipole moment (EDM) of neutrons, mercury (^{199}Hg) atomic comagnetometry [21,22] has been instrumental in perfecting the ultracold neutron technique [23] and achieving record sensitivity [24]. (For other applications of atomic comagnetometry beyond EDM searches, see Refs. [25–27] and references therein.)

A related example of high-precision BSM physics is the search for the EDM of charged particles, where the observable is a spin-flip frequency and the EDM-driven spin rotation signal must be accumulated during a long spin coherence time [10–14,28]. In this case, comagnetometry to maintain a resonance between the high-frequency spin flipper and the spin precession can be performed by measuring the precessing horizontal polarization of the stored beam when interacting with an internal polarimeter target. A Fourier analysis of the time-stamped events in the polarimeter allows to determine the oscillation frequency of the up-down asymmetry and thus the spin precession frequency with an accuracy of about 10^{-10} within a time window of 100 s (see Refs. [29,30] for details).

Our studies, however, revealed a non-negligible variation of the idle spin-precession frequency in the ring on the level of about $e - 8$ from one fill to another and during each fill (see Ref. [29], Fig. 4). In order to compensate for possible systematic biases for this unwanted drift of the magnetic fields in the storage ring and to maintain the spin-resonance condition, continuous comagnetometry is required to provide feedback to the rf spin flipper in terms of frequency and phase information. The feasibility of spin phase locking in the case of an idle precession of the horizontal polarization with an accuracy of 0.2 rad (rms) during the observation time of 90 s, corresponding to 6.95×10^7 beam revolutions in the ring, was experimentally demonstrated by the JEDI Collaboration [31,32]. However, when spins are closely aligned along the vertical axis in the machine during one or more spin flips, the horizontal polarization component disappears, making it impossible to control the spin-precession frequency beyond the quarter of the first spin-flip period.

The paper is organized as follows. Comagnetometry with a pilot bunch is discussed in Sec. II, the proof-of-principle concept of the experiment is presented in Sec. II A, with details of the modified driving circuit of the rf Wien filter (WF) and the fast rf switches in Sec. II B, and the characteristics of the signal and pilot bunches in the machine in Sec. II C. The experimental results are given in Sec. III. Spin flips in terms of exponential damping are discussed in Sec. III A, and,

based on the synchrotron oscillations formalism developed in the recent JEDI publication [33], in Sec. III C. A proposal for a spin flipper without Lorentz force as an application for future colliders is presented in Sec. IV, followed by the conclusions in Sec. V.

II. COMAGNETOMETRY WITH A PILOT BUNCH

In this paper we report on a single-species solution to the comagnetometry problem in continuous SFs based on the so-called pilot-bunch approach, for which we have successfully performed a proof-of-principle experiment at the Cooler Synchrotron (COSY) at Forschungszentrum Jülich, depicted in Fig. 1.

The demonstration was performed with polarized deuterons stored in the ring and accelerated to a flattop momentum of 970 MeV/c, and made use of an rf Wien filter, as a Lorentz force-free spin flipper [35,36]. The basic idea is to store multiple bunches of particles whose spins precess around the vertical guiding field of the ring dipole magnets. The rf WF is operated in a special mode in which it acts as a spin flipper for all but one bunch and is switched off once per beam revolution for a certain time interval when the bunch acting as a comagnetometer, the pilot bunch, passes the spin flipper.

A continuous feedback from the pilot bunch is used to maintain the spin-resonance condition of the rf WF. The details of this system are discussed in Ref. [37]. It should be noted that the applied pilot-bunch comagnetometry differs from the feedback applied in the earlier experiment [32], where the spin-precession frequency was kept constant by adjusting the beam orbital frequency without a spin rotator.

Pilot-bunch-based single-species comagnetometry in EDM searches with free precessing charged particles in storage rings differs significantly from the dual-species mercury (^{199}Hg) comagnetometry used in EDM searches with ultracold neutrons [21,22,24]. There, the signal neutrons and the comagnetometer mercury atoms are different species, both essentially at rest, with the mercury atoms probing the fields to which the neutrons are exposed, albeit suffering from a substantial vertical mismatch of the spatial distributions of the ultracold neutrons and warm mercury atoms [22,24,26]. Such a mismatch is common to dual-species comagnetometers. Furthermore, in two-species comagnetometry, the upper limit for the EDM of the neutrons can only be realized if the EDM of the comagnetometer atoms is known to be much smaller than that of the neutrons [21,22,24]. In our approach, however, the pilot bunch acts as a comagnetometer, probing the electromagnetic environment in the ring along the same path as the other bunches circulating in the ring. The key point about single-species comagnetometry in storage ring EDM experiments is that the EDM signal is contained in the SF frequency of the signal bunches exposed to the resonant rf fields of the spin flipper [28,33], while the pilot bunch is not affected at all because the spin flipper is turned off when the pilot bunch passes through.

While the present work focused primarily on comagnetometry, a much broader range of rf gating applications is conceivable. In particular, rf gating of spin flippers opens up the possibility of reversing the polarization of selected

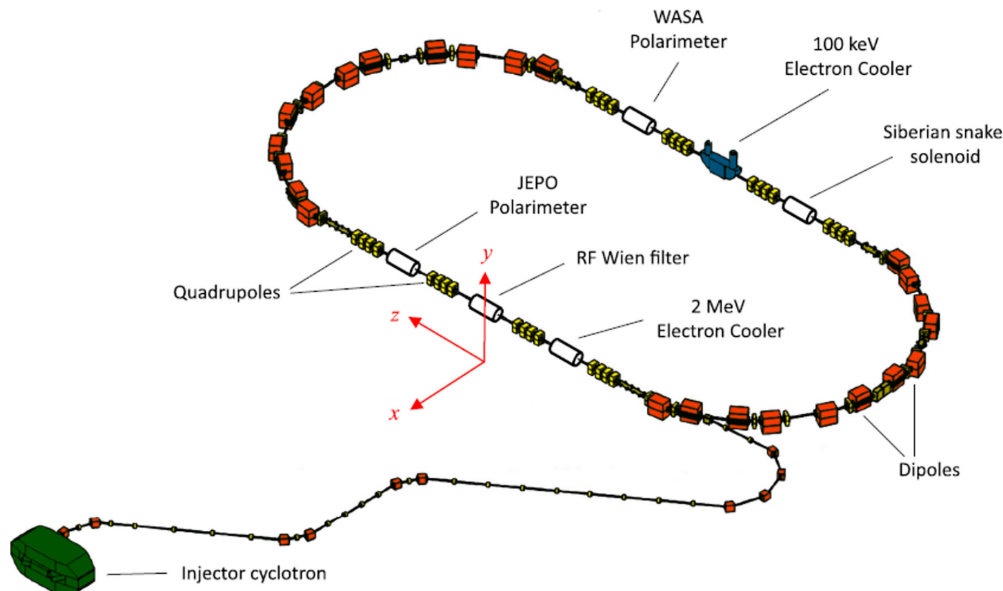


FIG. 1. Schematic diagram of the Cooler Synchrotron COSY as an example of a storage ring with rf Wien filter used as a spin flipper, located in front of the JEPO polarimeter. The machine parameters for the ring operation with polarized deuterons are listed in Table I. (Figure taken from Ref. [34] and slightly modified.)

bunches during each store, allowing us to organize successive bunches or trains of bunches with alternating vertical beam polarizations. This can lead to a significant reduction of systematic errors of spin observables at future colliders such as NICA (Nuclotron-based Ion Collider facility in Dubna [38]) and EIC (Electron-Ion Collider in Brookhaven [8]), as it will be possible to measure asymmetries with alternating polarizations using the same pair of colliding bunches, while currently only asymmetries from different bunches can be used to extract the spin observables.

A. Proof-of-principle experiment

The proof-of-principle of the pilot-bunch approach for co-magnetometry was demonstrated as follows. At each filling of the ring, vector-polarized deuterons were injected, bunched into two batches of about 10^9 particles separated by half a ring, electron cooled for about one minute at a beam kinetic energy of 76 MeV to a momentum spread of $\Delta p/p \approx 10^{-4}$, and then accelerated to the flattop momentum.

The spin-resonance frequency required to rotate the initial vertical spins of the stored deuterons was determined by Froissart-Stora scans [39] in which the frequency of the LC-resonant rf solenoid (Ref. [11], Sec. 7.7.3) was ramped across the expected resonance location to observe the point at which the vertical polarization p_y disappears in the polarimeter. In the subsequent measurements with vertical polarization, this frequency was then used to operate the rf WF. For the proof-of-principle experiment described here, satisfying the exact resonance condition is not mandatory (see Ref. [33], Sec. III A) for a discussion of the off-resonance regime).

The time distribution of the events recorded in the polarimeter is mapped into the revolution phase ϕ , given by

$$\phi = 2\pi [f_{rev}t_{cyc} - \text{int}(f_{rev}t_{cyc})] \in [0, 2\pi], \quad (1)$$

where 2π corresponds to the ring circumference. The evolution of the distribution of revolution phases of the two stored bunches as function of time in the cycle is shown in Fig. 2.

The projection near the midpoint of the cycle at $t_{cyc} = 122$ s is depicted in Fig. 3 yielding the longitudinal beam profile of pilot (p) and signal (s) bunches as a function of the revolution phase ϕ . The bunch length is increasing due to emittance growth. However, the gate width is well sufficient to fully shield the pilot bunch from the rf field of the WF.

The beam and machine parameters, as well as the parameters for the operation of the rf WF on flattop, are summarized in Table I. The typical timing parameters of the setup of the experiment in the accelerator are listed in Table II. The relative timing of events is measured by atomic clocks.

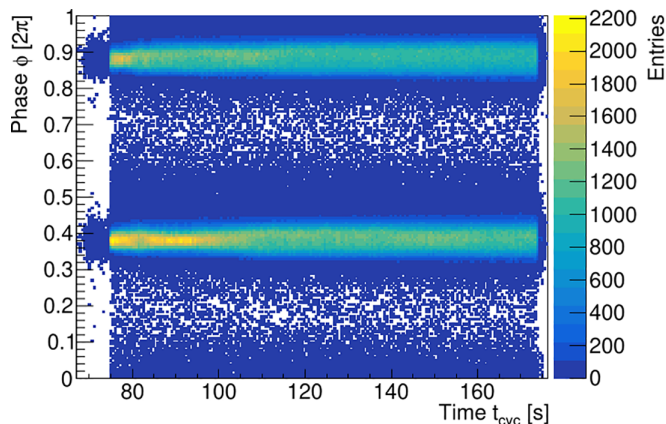


FIG. 2. The pilot bunch is located near a phase of $\phi_p \simeq 2.4$ rad and the signal bunch near $\phi_s \simeq 5.6$ rad (2π denotes the ring circumference).

TABLE I. Parameters of the deuteron kinematics, the COSY ring, the deuteron elementary quantities, and the field integrals of the rf Wien filter. The deuteron mass m and the deuteron g factor, taken from the NIST database [40], are used to specify G . The last column indicates whether the value is an input, calculated or measured.

Parameter	Symbol [Unit]	Value	Type
Deuteron momentum (lab)	P [MeV/c]	970.663702	calculated
Deuteron kinetic energy (lab)	T [MeV]	236.284783	calculated
Lorentz factor	γ [1]	1.125977	calculated
Beam velocity	β [c]	0.459617	calculated
Nominal COSY orbit circumference	ℓ_{COSY} [m]	183.572	input
Revolution frequency	f_{rev} [Hz]	50602.6	input
Spin precession frequency $f_s = G\gamma f_{\text{rev}}$	f_s [Hz]	-120847.303520	calculated
Deuteron mass	m [MeV]	1875.612793	input [[40], 2020]
Deuteron g factor	g [1]	1.714025	input [[40], 2020]
Deuteron $G = (g - 2)/2$	G [1]	-0.142987	calculated
Slip factor	η [1]	0.6545	measured
Momentum spread in middle of cycle	$\Delta p/p$ [1]	7.397×10^{-5}	measured
Synchrotron oscillation frequency	f_{sync} [Hz]	205 ± 21	measured
rf Wien filter electric field integral	$\int E_x^{\text{WF}} ds$ [V]	763.29509	calculated
rf Wien filter magnetic field integral	$\int B_y^{\text{WF}} ds$ [μTM]	5.65567704	calculated
rf Wien filter active length	ℓ_{WF} [m]	1.550	input

B. rf Wien filter

In a ring without magnetic imperfections, the spin-precession frequency is given by

$$f_s = G\gamma f_{\text{rev}}, \tag{2}$$

where G is the magnetic anomaly and γ the relativistic factor. In practice, magnetic ring imperfections will modify f_s significantly, as shown in Ref. [41]. The resonance condition for the rf WF is given by $f_{\text{WF}} = f_s + K f_{\text{rev}}$, where $K \in \mathbb{Z}$ and f_{rev} is the beam revolution frequency. During the experiment, the rf WF was operated at the sideband $K = -1$, and the fact that the resonance condition was not exactly met is of minor importance for the proof-of-principle experiment, described here.

In the experiment, the rf WF is operated in gated mode with two stored bunches, where the fast rf switches were included

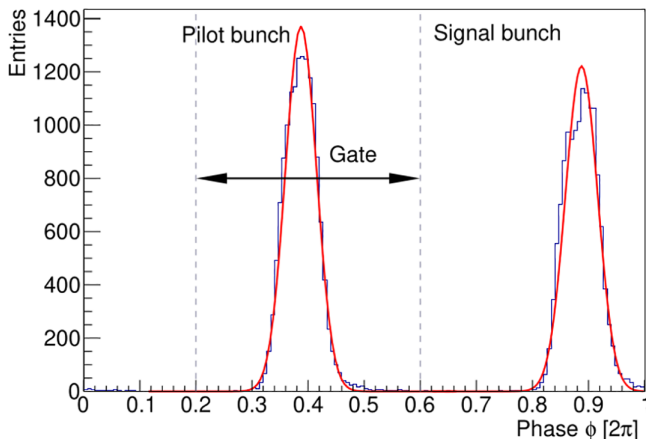


FIG. 3. Longitudinal beam profiles of two bunches, separated by a half-ring, plotted as a function of the revolution phase of Fig. 2 at $t_{\text{cyc}} = 122$ s in the cycle. The total number of entries included corresponds to ≈ 38000 events. The vertical lines indicate the gate width used to mask the pilot bunch from the rf of the Wien filter.

in the driving circuit, as shown in Fig. 4. After switching off the electron cooling at a time in the store of $t_{\text{cyc}} = 77$ s, the periphery of the beam is brought into interaction with the JEDI polarimeter target [42] by stochastic heating using a strip line in order to monitor the horizontal and vertical polarization components p_x and p_y of the beam.

In order to gate out one of the stored beam bunches, high-speed, high-power rf switches, integrated into the driving circuit [36] of the rf WF [35], were developed in close collaboration with the company Barthel [43] that had also built the rf power amplifiers and the components for the driving circuit. The switches are characterized by a symmetric switch on and off speed of 20 ns and are capable to handle 250 W of rf power, allowing the WF with four input ports to be operated close to 1 kW of total power. It should be noted that such a high switching speed cannot be achieved with a resonant circuit, for instance in an rf solenoid, which is often used as an rf spin flipper in storage rings. The switches are sophisticated, non-commercial, custom-designed active devices, composed of input and output matching circuits, switching high-electron-

TABLE II. Timing parameters for the machine operation to provide the beam parameters during the experiments (listed in Table I).

Event in cycle	Time [s]
Injection	0
Acceleration to flat-top momentum finished	2
Electron cooling on	3
Electron cooling off	50
Electron cooler magnets off	55
Carbon target moved in	60
White noise stochastic extraction on	68
Data acquisition on	68
rf Wien filter on	85
White noise stochastic extraction off	174
End of data taking	174

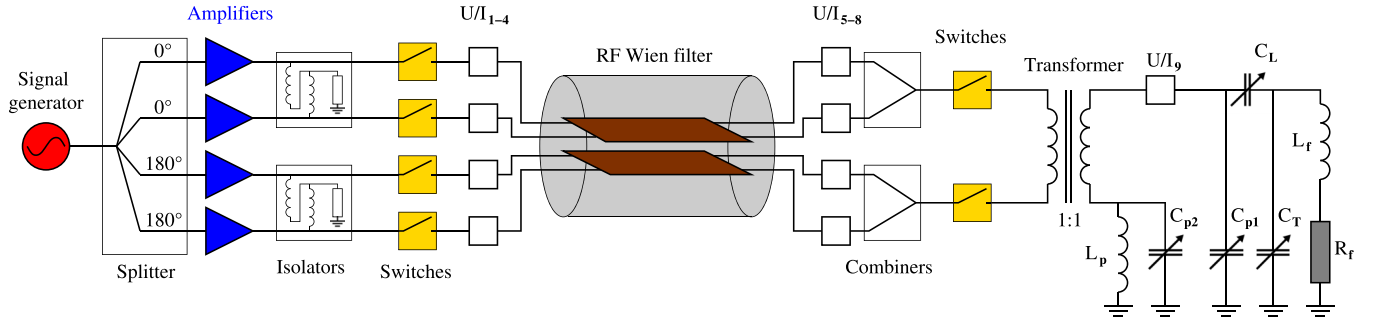


FIG. 4. Schematic of the driving circuit of the waveguide rf Wien filter, taken from Ref. [36], Fig. 1. The six fast rf switches, which were added to perform the experiments, are indicated in yellow.

mobility transistors (HEMTs), high-current driving circuits of these transistors and high-power and heat dissipation systems.

The modification of the driving circuit of the rf WF for the present experiment included the additional implementation of six identical fast rf switches, as shown in yellow in Fig. 4. The signal from an rf generator [44] is fed into four rf amplifiers via a 1:4 signal splitter and routed into the waveguide. The purpose of the tunable elements in the driving circuit is to adjust the device so that the Lorentz force on the circulating particles can be minimized [34]. Four switches are installed in each of the four input ports, and two switches at the output of the waveguide of the WF behind the power combiners.

The rf switches are operated at the beam revolution frequency and render the rf fields of the WF invisible to the pilot bunch, while the signal bunch is subjected to rf-driven multiple spin flips. As shown in Fig. 3, the rf switches are synchronized with the pilot bunches, so that the center of the gate is located at $\phi = \phi_p$ [see Eq. (3) and Table III]. The pattern of electromagnetic field suppression in the rf WF by the rf switches is shown in Fig. 5; the switches were operated at $f_{rev} = 750602.6$ Hz. The data shown were recorded during a test run without circulating beam.

C. Characteristics of signal and pilot bunches

After switching off electron cooling, the lengths of pilot and signal bunch increase by about 60–80 % during the cycle. To quantify this increase, the observed longitudinal beam profiles of pilot (p) and signal (s) bunches, shown in Fig. 3 in terms of the revolution phase, defined by Eq. (1), were approximated by Gaussians,

$$\frac{dN_{p,s}}{d\phi} \propto \exp\left(-\frac{(\phi - \phi_{p,s})^2}{2\sigma_{p,s}^2}\right). \quad (3)$$

TABLE III. Results from fits with Gaussians, yielding for pilot (p) and signal (s) bunch the azimuthal locations $\phi_{p,s}$ and widths $\sigma_{p,s}$ at three times t_{cyc} during a typical cycle, shown in Fig. 3. The last column shows the separation of the signal and pilot bunches in units of the mean total 4σ bunch width.

Time t_{cyc} [s]	pilot bunch		signal bunch		bunch separation $\frac{\phi_s - \phi_p}{2(\sigma_s + \sigma_p)}$
	ϕ_p [rad]	$2\sigma_p$ [rad]	ϕ_s [rad]	$2\sigma_s$ [rad]	
78	2.4198 ± 0.0012	0.2742 ± 0.0017	5.5586 ± 0.0013	0.2840 ± 0.0017	5.6
122	2.4339 ± 0.0015	0.3483 ± 0.0019	5.5770 ± 0.0016	0.3635 ± 0.0020	4.5
173	2.4288 ± 0.0016	0.3823 ± 0.0023	5.5745 ± 0.0018	0.4057 ± 0.0022	4.0

The fitting results at the beginning, middle, and end of the cycle are listed in Table III. During a cycle, at the 2σ level, the fractional bunch length increases from 7–13 % with respect to the ring circumference. The two bunches are well separated, as can be seen from the last column in Table III showing the separation of the signal and pilot bunches, expressed as the ratio of the differences in azimuthal locations to the mean total 4σ bunch width.

The temporal gate duration amounts to $T_G = 0.556$ μ s, while the particle revolution time is $T_{rev} = 1.33$ μ s, and in terms of the beam revolution phase, the gate width is $\Delta\phi = 2\pi f_{rev} T_G = 2.62$ rad. Relative to the width σ_p of the beam (listed in Table III), the gate width $\Delta\phi$ varies from $19\sigma_p$ at the beginning of the cycle to $14\sigma_p$ at the end and is thus entirely sufficient for the pilot bunch to pass through the rf WF unaffected while it is switched off.

III. EXPERIMENTAL RESULTS

The function of the pilot bunch as a comagnetometer derives from its insensitivity to the operation of the WF, so that its polarization continues to idly precess in the ring plane, thus continuously providing information about the spin precession. This information can be used to correct the frequency of the rf WF to maintain the resonance condition, and the feedback system that enables this is discussed in detail in Ref. [37]. The task of the present experiment, however, was rather a demonstration of the technique as a proof of principle, and a characterization of the spin-flip behavior of the signal and pilot bunches. The experiment was conducted using vertical polarization of deuterons, therefore spin-frequency feedback from the precessing horizontal polarization could not be applied. Instead, in the EDM experiments we have performed,

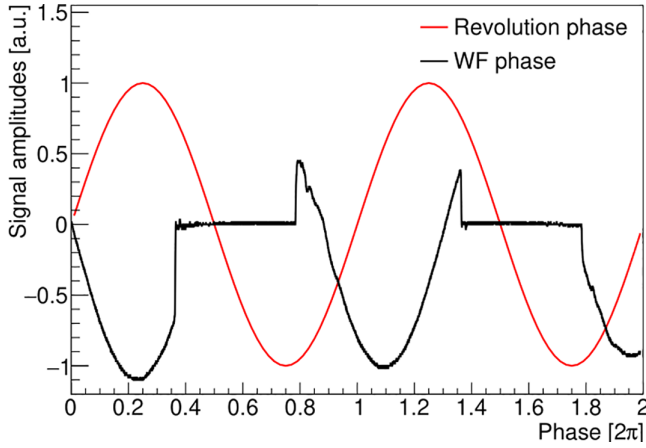


FIG. 5. The signal amplitude of the field in the rf Wien filter, shown in black, measured during one of the dedicated test runs without circulating beam. The sine of the revolution phase, shown in red, is plotted to emphasize the phase locking of the gate with vanishing fields in the WF to the beam revolutions.

the spin-precession frequency measurement of the pilot-bunch data allowed to keep the rf WF on resonance.

The experimental result of the test of the pilot-bunch principle is illustrated in Fig. 6. Recording the time stamp of the interactions in the detectors of the polarimeter enables the simultaneous measurements of the left-right count rate asymmetries caused by the pilot and signal bunches, which were not corrected for acceptance effects.

It should be noted that for the experimental proof of the pilot-bunch technique aimed at here, only asymmetries need to be taken into account; calibrated polarizations are not required. As the target intercepts the periphery of the beam, the off-centered interactions induce a finite offset of the measured asymmetries and also exhibit a slow time dependence caused by the enhanced beam heating to maintain a constant count

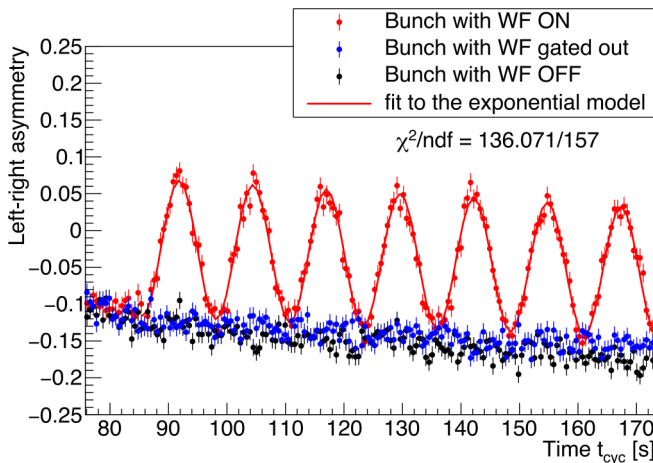


FIG. 6. Left-right asymmetry in the polarimeter, caused by the oscillating vertical polarization of the signal (red dots) and the simultaneously recorded pilot bunch (blue dots). The black dots are for a cycle with the rf Wien filter completely turned off. The red line shows a fit with Eq. (4) using events within the $\pm 2\sigma_s$ limit of the signal bunch distribution (see Fig. 3).

TABLE IV. Parameters of a fit to the oscillation pattern of the left-right signal bunch asymmetry, shown in Fig. 6, with the exponential function $A(t)$, given in Eq. (4). The $\chi^2/\text{ndf} = 136.071/157 = 0.87$.

Parameter	Value	Error	Unit
a_s	-4.04	0.38	10^{-4}s^{-1}
t_0	85.548	0.060	s
b_s	-0.0228	0.0019	1
d_s	-0.0936	0.0027	1
Γ_s	7.30	5.86	10^{-4}s^{-1}
f_{SF}	0.07944	0.00010	Hz

rate, but these are arguably independent of the beam polarization and would not affect the principal distinction between the pilot and signal bunches.

A. Exponential damping

The oscillation pattern of the asymmetry in the polarimeter caused by the vertical polarization of the signal bunch was fitted using data within the $\pm 2\sigma$ limit of the bunch distribution, as shown in Fig. 6. The signal bunch (red symbols) exhibits the expected multiple continuous spin flips (SF). In the phenomenological analysis, following Bloch [45], the oscillations of the observed beam-spin asymmetries of the signal bunch were fitted by the function

$$A_s(t) = a_s(t - t_0) + b_s + d_s \exp[-\Gamma_s(t - t_0)] \times \cos[2\pi f_{\text{SF}}(t - t_0)], \quad (4)$$

where an allowance is made for the exponential damping caused by spin decoherence in terms of the time constant $\tau_s = 1/\Gamma_s$.

Our convention is to assign an initial spin-flip phase of zero, which leads to a negative initial spin asymmetry $d_{p,s}$ and means that the rf WF was effectively turned on at a cycle time of $t_0 \approx 85.5$ s. The fit results are summarized in Table IV. The first two terms, $a_s(t - t_0) + b_s$, describe the aforementioned time-dependent offset of the left-right asymmetry, the other terms parametrize the spin-flip amplitude d_s , the spin-flip frequency f_{SF} , and the very small damping constant Γ_s , with good fit quality, expressed as χ^2 per number of degrees of freedom (ndf), of $\chi^2/\text{ndf} = 136.07/157$.

Multiple spin flips are often described in terms of the efficiency ϵ_{flip} , i.e., by the ratio of polarizations after and before a single spin flip (see, e.g., Refs. [5–7]). In terms of our parametrization in Eq. (4) and the values from Table IV, the spin-flip efficiency in our experiment can be expressed via

$$\epsilon_{\text{SF}} = 1 - \frac{\Gamma_s}{2f_{\text{SF}}} = 0.9954 \pm 0.0037. \quad (5)$$

The total polarization loss after the 14 spin flips shown in Fig. 6 amounts to

$$\frac{\Delta P}{P} = 0.062 \pm 0.050. \quad (6)$$

The observed beam loss during the 90-s spin-flip cycle was about 45%.

TABLE V. Parameters of fits to the oscillation pattern of the left-right pilot-bunch asymmetry, a_p , b_p , d_p , and of asymmetry in the WF-off fill, a_0 , b_0 , d_0 , shown in Fig. 6, using a truncated version of $A(t)$ from Eq. (4), where the parameters t_0 , Γ_s , and f_{SF} are fixed to the values obtained from the fit to the signal bunch, listed in Table IV. For the pilot bunch $\chi^2/\text{ndf} = 131.483/160 = 0.82$, for the WF-off bunch $\chi^2/\text{ndf} = 155.743/162 = 0.96$.

Parameter	Value	Error	Unit
a_p	-4.10	0.36	10^{-4}s^{-1}
b_p	-0.1230	0.0018	1
d_p	-0.00074	0.00127	1
a_0	-5.53	0.36	10^{-4}s^{-1}
b_0	-0.1295	0.0018	1
d_0	-0.00292	0.00135	1

In the present experiment, the observed attenuation of the polarization amplitude proved to be very weak, and the resulting single spin-flip efficiency is essentially compatible with unity. In striking contrast, the asymmetry measured for the pilot bunch (blue symbols in Fig. 6) shows no oscillation signal at the spin-flip frequency f_{SF} and perfectly matches the signal from a cycle where the WF was switched off (black symbols), with the caveat that here we compare data from different fills.

To identify a remaining polarization oscillation in the pilot bunch, a fit to the oscillation pattern of the left-right pilot-bunch asymmetry and to the asymmetry from the fill with rf WF switched off is performed using a truncated version of the function $A(t)$ in Eq. (4), where t_0 and f_{SF} are fixed to the values obtained for the signal bunch (see Table IV). In view of the vanishing sensitivity to the damping parameter, we set in addition $\Gamma_p = \Gamma_s$, so that the set of fixed parameters to fit the pilot bunch is: t_0 , f_{SF} , and $\Gamma_p = \Gamma_s$. The fitted parameters are summarized in Table V. The fitted oscillation amplitudes of the pilot bunch and of the WF-off bunch, d_p and d_0 , are consistent with zero. The signal and the pilot bunch are expected to have the same initial polarization. Thus, we expect the relationship $b_p = d_s + b_s$ to hold. Substituting the values, we find $b_p = -0.123 \pm 0.002$ and $d_s + b_s = -0.116 \pm 0.003$. These values agree within a 2-sigma range and thus confirm the expectation.

Using the fitted values values for d_s and d_p from Tables IV and V, the efficiency of the gate, expressed via

$$\epsilon_{\text{gate}} = 1 - \frac{d_p}{d_s} = 0.9921 \pm 0.0136, \quad (7)$$

is compatible with unity, indicating that our fast prototype rf switches were operating as desired, providing full screening of the pilot bunch from the rf WF fields.

B. Frequency detuning of the rf Wien filter

It is instructive to compare the fitted signal-bunch spin-flip frequency f_{SF} to the expectation from the numerically calculated field maps of the WF magnetic field integral, given in Table I. In the case of an ideal resonance for the conditions of the present experiment, one finds $f_{\text{SF}}^{(\text{WF})} = 7.694 \times 10^{-2}$ Hz [Ref. [41], Eq. (13)], which is by about 3% smaller than the fit-

ted result for f_{SF} in Table IV. We recall that in our experiment the operation frequency of the rf WF was determined from Froissart-Stora scans [39] of the frequency of the rf solenoid, and no feedback has been imposed to correct for the potential deviation from the exact resonance during the further spin flips by the rf WF.

According to the formalism, presented in Ref. [33], Sec. II C, Eq. (33), detuning enhances the spin-flip frequency,

$$f_{\text{SF}}^2 = (f_{\text{SF}}^{(\text{WF})})^2 + (\Delta f_s)^2, \quad (8)$$

where Δf_s denotes the frequency detuning of the signal (s) bunch. Suppressing a possible systematic uncertainty of the calculated WF field integral, we find rather weak detuning of

$$\begin{aligned} \Delta f_s &= (0.020 \pm 0.004_{\text{stat}}) \text{ Hz} \\ &\approx 2.7 \times 10^{-8} f_{\text{rev}} \\ &\approx -2.3 \times 10^{-8} f_{\text{WF}}. \end{aligned} \quad (9)$$

Another manifestation of detuning is an incomplete spin flip, described by the precession of the spin envelope. Exactly on resonance, the spin envelope precesses around the radial magnetic field of the WF. Detuning causes an upward or downward deviation from the radial orientation of the precession axis \vec{m} of the spin envelope, by an angle $\rho = \arccos(\Delta f_s/f_{\text{SF}})$ [Ref. [33], Sec. II C, Eq. (29)]. The initial polarization $\vec{S}(t_0) = S_s(0)\vec{e}_s$ points along the spin stable axis of the idle precession \vec{e}_s , and its evolution can be cast in the form [Ref. [33], Sec. III C, Eq. (36)]

$$\begin{aligned} \frac{S_s(t)}{S_s(0)} &= \cos^2 \rho + \sin^2 \rho \cos [2\pi f_{\text{SF}}(t - t_0)] \\ &= \left(\frac{\Delta f_s}{f_{\text{SF}}}\right)^2 + \left[1 - \left(\frac{\Delta f_s}{f_{\text{SF}}}\right)^2\right] \cos [2\pi f_{\text{SF}}(t - t_0)]. \end{aligned} \quad (10)$$

Since the main purpose of this experiment was to prove the principle of pilot-bunch comagnetometry, these systematic effects will not be further discussed here.

C. Damping based on synchrotron oscillations

To a certain extent, synchrotron oscillations in the stored beam can contribute to a synchrotron amplitude-dependent detuning of the spin-flip oscillations of the central region compared to the head and tail region of the beam bunch. Particles in the bunch are in constant synchrotron (sy) motion. Evidently, only particles with sufficiently large synchrotron amplitudes contribute to the head and tail portions of the bunch. These particles keep oscillating from head to tail and vice versa, spending part of their time also in the central portion of the bunch. Synchrotron oscillations modulate the spin-precession frequency and can affect the spin-flip frequency as well [33]. Aspects of the longitudinal phase-space dependence of the beam polarization are discussed in great detail in Ref. [33] (see also the RHIC results on the radial phase-space tomography of polarization in Ref. [46] and their discussion in Ref. [47]).

As a spinoff of our data, we are in the position to investigate for the first time the dependence of the spin-flip dynamics

TABLE VI. Parameters obtained from fitting the left-right asymmetry of the oscillation pattern of the signal bunch in Fig. 6 with the synchrotron oscillations model, described by Eq. (11). The $\chi^2/\text{ndf} = 136.936/158 = 0.87$.

Parameter	Central events inside the $[-2, 2]\sigma_s$ cut	Unit
a_{sy}	-4.01 ± 0.38	10^{-4}s^{-1}
b_{sy}	-0.02967 ± 0.00191	1
d_{sy}	-0.092419 ± 0.002046	1
Q_{sy}	0.007728 ± 0.003602	1
$f_{\text{SF}}^{(\text{sy})}$	0.079984 ± 0.000278	Hz

on the synchrotron oscillation (SO) amplitude. According to the discussion in Ref. [33], in the approximation of the synchrotron oscillation-dominated spin decoherence, the evolution of the spin asymmetry is described by the function

$$A_{\text{sy}}(t) = a_{\text{sy}}(t - t_0) + b_{\text{sy}} + \frac{d_{\text{sy}}}{\sqrt{1 + [2\pi Q_{\text{sy}} f_{\text{SF}}^{(\text{sy})}(t - t_0)]^2}} \times \cos [2\pi f_{\text{SF}}^{(\text{sy})}(t - t_0) - \arctan (2\pi Q_{\text{sy}} f_{\text{SF}}^{(\text{sy})}(t - t_0))], \quad (11)$$

which unlike Eq. (4) does not contain an exponential damping. The nonexponential depolarization parameter is given by

$$Q_{\text{sy}} = \frac{1}{2}(K + G\gamma)^2 \langle \phi_s^2 \rangle. \quad (12)$$

The present data were taken at the side band $K = -1$. For the all inclusive bunch $\langle \phi_s^2 \rangle = \sigma_s^2$, and for the midcycle with $\sigma_s = 0.18$ from Table III, we expect $Q_{\text{sy}} \approx 0.022$. For the signal bunch with the basic $\pm 2\sigma_s$ boundaries, a crude estimation with the Gaussian approximation of the bunch profile yields $\langle \phi_s^2 \rangle \approx 0.4\sigma_s^2$. Our expectation from Eq. (12) is $Q_{\text{sy}}(\pm 2\sigma_s) \approx 0.009$, which is in the ballpark of the fit result, obtained with A_{sy} from Eq. (11) (listed in Table VI). The corresponding polarization loss after 14 spin flips, given by

$$\frac{\Delta P}{P} \approx \frac{1}{2}(14\pi Q_{\text{sy}})^2 = 0.058_{-0.041}^{+0.066}, \quad (13)$$

is consistent with the exponential parametrization in Eq. (6).

1. Synchrotron oscillations and spin-flip frequency

The comparison of the oscillation amplitudes and offset parameters for the SO and the exponential damping model show excellent agreement, i.e., identical results within the error bars, also regarding the $\chi^2/\text{ndf} = 0.87$. The SO fit results to the data shown in Fig. 6, summarized in Table VI, are virtually indistinguishable from the exponential curve, given in Table IV. As was already observed with the exponential parametrization, the depolarization parameter Q_{sy} is a 2σ effect. In the dynamical SO model, the nonexponential damping entails the nonlinear spin-flip phase walk from the arctangent term, but with very small magnitude of the fitted Q_{sy} the linear approximation holds, $\arctan[2\pi Q_{\text{sy}} f_{\text{SF}}^{(\text{sy})}(t - t_0)] \approx 2\pi Q_{\text{sy}} f_{\text{SF}}^{(\text{sy})}(t - t_0)$. The resulting effective spin-flip frequency $f_{\text{SF}}^{(\text{eff})} = f_{\text{SF}}^{(\text{sy})}(1 - Q_{\text{sy}})$ must be compared to that of the exponential model $f_{\text{SF}}^{(\text{exp})}$, given in Table IV. We expect that $\Delta f_{\text{SF}} = f_{\text{SF}}^{(\text{sy})} - f_{\text{SF}}^{(\text{exp})} = Q_{\text{sy}} f_{\text{SF}}^{(\text{sy})} =$

$(6.2 \pm 2.9) \times 10^{-4}$ Hz, which should be compared to the observed difference $(4.0 \pm 2.8) \times 10^{-4}$ Hz from the fit results, indicating agreement within the uncertainties.

2. Spin flips of central vs head and tail particles

We would like to address here the question whether the head and tail portions of the signal bunches exhibit a difference regarding the observed spin-flip properties compared to the central region. To this end, fits were performed with the function $A_{\text{sy}}(t)$, separately for the data within the central region of the bunch distribution using Set I ($\phi_s \in [-0.6, +0.6]\sigma_s$) and to the head and tail region using Set II ($\phi_s \in [-2, -0.6]\sigma_s \vee \phi_s \in [+0.6, +2]\sigma_s$). The separation of the two sets was chosen to provide statistically independent data samples of about equal number of recorded events. Note that particles with synchrotron amplitudes below $0.6\sigma_s$ do not contribute to the head and tail Set II. However, in the course of the synchrotron oscillations, particles with larger synchrotron amplitudes populating Set II, will spend part of their time in Set I [33].

The fitted oscillation frequencies compare as follows: $f_{\text{SF}}^{(\text{sy})\text{I+II}} = (79.98 \pm 0.28) \times 10^{-3}$ Hz (see Table VII) vs $f_{\text{SF}}^{(\text{sy})\text{I}} = (80.09 \pm 0.36) \times 10^{-3}$ Hz and $f_{\text{SF}}^{(\text{sy})\text{II}} = (79.73 \pm 0.80) \times 10^{-3}$ Hz (see Table VII). The results for the SO depolarization parameters read $Q_{\text{sy}}^{\text{I+II}} = (7.73 \pm 3.60) \times 10^{-3}$ vs $Q_{\text{sy}}^{\text{I}} = (9.23 \pm 4.61) \times 10^{-3}$ and $Q_{\text{sy}}^{\text{II}} = (3.69 \pm 10.23) \times 10^{-3}$. We observe no statistically significant trends.

Unlike the spin-flip frequency and polarization attenuation, the spin-flip amplitude is sensitive to the nonuniform longitudinal polarization profile. Our results for the oscillation amplitudes, $d_{\text{sy}}^{\text{I+II}} = (-9.24 \pm 0.20) \times 10^{-2}$ (Table VI) vs $d_{\text{sy}}^{\text{I}} = (-9.39 \pm 0.29) \times 10^{-2}$ and $d_{\text{sy}}^{\text{II}} = (-8.82 \pm 0.30) \times 10^{-2}$ (Table VII), show no significant trends within the present error bars. The observed beam loss by about 45% during the 90-s spin-flip cycle could have changed the peripheral-to-core composition of polarization of the beam.

Our analysis suggests noticeable differences between the central (Set I) and the head and tail (Set II) regions of the signal bunch in terms of the offset parameters a_{sy} and b_{sy} of the polarimeter asymmetry, listed in Table VII. The fit to the full data within the 2σ bunch boundary yielded a value for the initial asymmetry offset $b_{\text{sy}}^{\text{I+II}} = (-2.97 \pm 0.19) \times 10^{-2}$ (see Table VI), while we found for the central part $b_{\text{sy}}^{\text{I}} = (-0.62 \pm 0.26) \times 10^{-2}$ and for the head and tail regions $b_{\text{sy}}^{\text{II}} = (-2.70 \pm 0.29) \times 10^{-2}$ (see Table VII), which suggest that the initial offset b_{sy} is dominated by the head and tail region of the bunch. The related results for the offset slope parameter are $a_{\text{sy}}^{\text{I+II}} = -(4.01 \pm 0.38) \times 10^{-4}$ (see Table VI) vs $a_{\text{sy}}^{\text{I}} = (-6.55 \pm 0.55) \times 10^{-4}$ for the central part and $a_{\text{sy}}^{\text{II}} = (-0.61 \pm 0.56) \times 10^{-4}$ for the head and tail regions. Barring a drift of the storage ring parameters during the experiments, it is tempting to attribute the observed walk of the offset to stochastic heating of the beam to maintain about the same event rate in the polarimeter. Within this picture, heating has a stronger impact on the central region of the bunch. Regardless of these speculations, the above results can be regarded as longitudinal tomography of beam bunches, which may be of

TABLE VII. Parameters obtained from fits to the left-right signal bunch asymmetry of the oscillation pattern with the synchrotron oscillations model described by Eq. (11) to the central Set I and the head and tail Set II.

Parameter	Central Set I $\phi_s \in [-0.6, 0.6]\sigma_s$	Head and tail Set II $\phi_s \in [-2, -0.6]\sigma_s \vee \phi_s \in [+0.6, +2]\sigma_s$	Unit
a_{sy}	-6.55 ± 0.55	-0.61 ± 0.56	10^{-4}s^{-1}
b_{sy}	-0.006213 ± 0.002637	-0.02700 ± 0.00291	1
d_{sy}	-0.093915 ± 0.002885	-0.0881996 ± 0.002987	1
Q_{sy}	0.009227 ± 0.004616	0.003689 ± 0.010229	1
$f_{SF}^{(sy)}$	0.080093 ± 0.0003581	0.079730 ± 0.000811	Hz
χ^2/ndf	$179.821/158 = 1.14$	$132.685/158 = 0.84$	1

interest for the determination of the luminosity in colliders, for example.

IV. SPIN FLIPPER WITHOUT LORENTZ FORCE

Our technique of using a Lorentz force-free rf WF operating at a fixed frequency as a spin manipulator has the potential to open new possibilities for spin physics experiments at future accelerators such as the EIC and NICA. In terms of continuous spin flips, such a device does not suffer from the limitations of the Froissart-Stora scanning technique [39], employed at the RHIC spin flipper using rf dipoles [48,49] and can be tuned to minimize adverse effects on the beam orbit [34], produced by rf dipoles and rf solenoids. Instead of injecting polarized bunches with a predefined alternating polarization pattern into the collider, one can inject one polarization state and invert the vertical polarization by selective gating on individual bunches or on trains of bunches on flattop.

As the rate of spin flip of an rf WF scales with the inverse energy squared [Ref. [41], Eq. (13)], however, to obtain similar spin flip rates as in our experiment, such a device for EIC (275 GeV, $\gamma \approx 295$, $f_{\text{rev}} \approx 78$ kHz) would require rf fields increased by a factor of $\gamma^2 \approx 8.7 \times 10^4$. With a 10 m long rf WF at sideband $K = 15000$, frequency $f_{\text{WF}} \approx 1.1$ GHz, driven by a 1 MW amplifier [50], spin flip periods of one minute appear feasible for protons. Regarding the prospects for gating out an individual bunch with an rf WF at EIC, we note that the rf switches used in the present experiment already provide switching times of ≈ 2 ns, while at EIC with $n_b \approx 1180$ bunches, the bunch period will be $(f_{\text{rev}} \cdot n_b)^{-1} \approx 11$ ns. Thus, the achieved switching time is already in the ballpark of the EIC requirements, but handling the considerably higher power will require a dedicated development effort.

V. CONCLUSION

To summarize, we demonstrated the feasibility of pilot-bunch-based single-species comagnetometry for storage ring experiments using an rf WF equipped with fast rf switches. Our approach is primarily motivated by precision spin ex-

periments that involve testing of fundamental symmetries, such as searches for the parity- and time-reversal invariance violating permanent EDMs of charged particles [10,11], but it may find other applications in the field of spin physics at storage rings. As an example, we mention in this context the search for millistrong CP violation [17–19] via the measurement of time reversal-odd spin asymmetries in interactions of tensor polarized deuterons with polarized protons, where the in-plane precessing spins of deuterons would give rise to a T -odd asymmetry that oscillates with twice the spin-precession frequency, free of systematics [20].

A related example of self-comagnetometry is the search for axions using polarized particles in storage rings as axion antennas [51]. If the Froissart-Stora scan were to provide experimental evidence of an axion resonance at a particular frequency, one could use the beam itself as a magnetometer to narrow the scan range and eventually stabilize the spin-precession frequency at the suspected axion field oscillation frequency, thereby enhancing the sensitivity to the axion signal.

ACKNOWLEDGMENTS

We would like to thank the COSY crew for their support in setting up the COSY accelerator for the experiment. We are grateful to V. Ptitsyn for illuminating discussions on the RHIC spin flipper. The work presented here has been performed in the framework of the JEDI Collaboration and was supported by an ERC Advanced Grant of the European Union (Proposal No. 694340: Search for electric dipole moments using storage rings) and by the Shota Rustaveli National Science Foundation of the Republic of Georgia (SRNSFG Grant No. DI-18-298: High precision polarimetry for charged particle EDM searches in storage rings). This research is part of a project that has received funding from the European Union's Horizon 2020 research and innovation program under grant agreement STRONG-2020 No. 824093. The work of A.A., A.M., and N.N.N. on the topic was supported by the Russian Science Foundation (Grant No. 22-42-04419). We would like to thank Matthias Barthel and his colleagues for developing, manufacturing and providing the fast rf switches for the experiment.

[1] F. Rathmann, B. v. Przewoski, W. A. Dezarn, J. Duskow, M. Dzemidzic, W. Haeberli, J. G. Hardie, B. Lorentz, H. O. Meyer, P. V. Pancella *et al.*, Complete angular distribution measure-

ments of pp spin correlation parameters A_{xx} , A_{yy} , and A_{xz} and analyzing power A_y at 197.4 MeV, *Phys. Rev. C* **58**, 658 (1998).

- [2] B. v. Przewoski, H. O. Meyer, J. T. Balewski, W. W. Daehnick, J. Doskow, W. Haerberli, R. Ibal, B. Lorentz, R. E. Pollock, P. V. Pancella *et al.*, Analyzing powers and spin correlation coefficients for $p + d$ elastic scattering at 135 and 200 MeV, *Phys. Rev. C* **74**, 064003 (2006).
- [3] S. Y. Lee, *Spin Dynamics and Snakes in Synchrotrons* (World Scientific, Singapore, 1997).
- [4] S. R. Mane, Y. M. Shatunov, and K. Yokoya, Spin-polarized charged particle beams in high-energy accelerators, *Rep. Prog. Phys.* **68**, 1997 (2005).
- [5] V. S. Morozov, Z. B. Etienne, M. C. Kandes, A. D. Krisch, M. A. Leonova, D. W. Sivers, V. K. Wong, K. Yonehara, V. A. Anferov, H. O. Meyer *et al.*, First spin flipping of a stored spin-1 polarized beam, *Phys. Rev. Lett.* **91**, 214801 (2003).
- [6] H.-O. Meyer, The Indiana Cooler: A retrospective, *Annu. Rev. Nucl. Part. Sci.* **57**, 1 (2007).
- [7] C. Weidemann, F. Rathmann, H. J. Stein, B. Lorentz, Z. Bagdasarian, L. Barion, S. Barsov, U. Bechstedt, S. Bertelli, D. Chiladze *et al.*, Toward polarized antiprotons: Machine development for spin-filtering experiments, *Phys. Rev. ST Accel. Beams* **18**, 020101 (2015).
- [8] R. Abdul Khalek, A. Accardi, J. Adam, D. Adamiak, W. Akers, M. Albaladejo, A. Al-bataineh, M. Alexeev, F. Ameli, P. Antonioli *et al.*, Science requirements and detector concepts for the electron-ion collider: EIC yellow report, *Nucl. Phys. A* **1026**, 122447 (2022).
- [9] D. P. Aguillard, T. Albahri, D. Allspach, A. Anisenkov, K. Badgley, S. Baeßler, I. Bailey, L. Bailey, V. A. Baranov, E. Barlas-Yucel *et al.*, The Muon $g - 2$ Collaboration, Measurement of the positive muon anomalous magnetic moment to 0.20 ppm, *Phys. Rev. Lett.* **131**, 161802 (2023).
- [10] V. Anastassopoulos, S. Andrianov, R. Baartman, S. Baessler, M. Bai, J. Benante, M. Berz, M. Blaskiewicz, T. Bowcock, K. Brown *et al.*, A storage ring experiment to detect a proton electric dipole moment, *Rev. Sci. Instrum.* **87**, 115116 (2016).
- [11] F. Abusaif *et al.* (CPEDM Collaboration), *Storage Ring to Search for Electric Dipole Moments of Charged Particles: Feasibility Study*, CERN Yellow Reports: Monographs, 2021-003 (CERN, Geneva, 2021).
- [12] I. A. Koop, in *Proceedings of the 4th International Particle Accelerator Conference (IPAC 2013): Shanghai, China, May 12–17, 2013*, edited by Z. Dai, C. Petit-Jean-Genaz, V. R. W. Schaa, and C. Zhang (JACoW, Geneva, Switzerland, 2013), JACoW conferences, p. TUPWO040.
- [13] S. Hacıömeroğlu and Y. K. Semertzidis, Hybrid ring design in the storage-ring proton electric dipole moment experiment, *Phys. Rev. Accel. Beams* **22**, 034001 (2019).
- [14] R. Alarcon, J. Alexander, V. Anastassopoulos, T. Aoki, R. Baartman, S. Baeßler, L. Bartoszek, D. H. Beck, F. Bedeschi, R. Berger *et al.*, Electric dipole moments and the search for new physics, [arXiv:2203.08103](https://arxiv.org/abs/2203.08103).
- [15] G. Cavoto, R. Chakraborty, A. Doinaki, C. Dutsov, M. Giovannozzi, T. Hume, K. Kirch, K. Michielsen, L. Morvaj, A. Papa *et al.*, Anomalous spin precession systematic effects in the search for a muon EDM using the frozen-spin technique, *Eur. Phys. J. C* **84**, 262 (2024).
- [16] M. Abe, S. Bae, G. Beer, G. Bunce, H. Choi, S. Choi, M. Chung, W. da Silva, S. Eidelman, M. Finger *et al.*, A new approach for measuring the muon anomalous magnetic moment and electric dipole moment, *Prog. Theor. Exp. Phys.* **2019**, 053C02 (2019).
- [17] L. B. Okun, Note concerning CP parity, *Sov. J. Nucl. Phys.* **1**, 670 (1965).
- [18] J. Prentki and M. J. G. Veltman, Possibility of CP violation in semistrong interactions, *Phys. Lett.* **15**, 88 (1965).
- [19] T. D. Lee and L. Wolfenstein, Analysis of CP noninvariant interactions and the K_1^0 , K_2^0 system, *Phys. Rev.* **138**, B1490 (1965).
- [20] N. Nikolaev, F. Rathmann, A. Silenko, and Y. Uzikov, New approach to search for parity-even and parity-odd time-reversal violation beyond the standard model in a storage ring, *Phys. Lett. B* **811**, 135983 (2020).
- [21] K. Green, P. Harris, P. Iaydjiev, D. May, J. Pendlebury, K. Smith, M. van der Grinten, P. Geltenbort, and S. Ivanov, Performance of an atomic mercury magnetometer in the neutron EDM experiment, *Nucl. Instrum. Meth. Phys. Res. A* **404**, 381 (1998).
- [22] J. M. Pendlebury, S. Afach, N. J. Ayres, C. A. Baker, G. Ban, G. Bison, K. Bodek, M. Burghoff, P. Geltenbort, K. Green *et al.*, Revised experimental upper limit on the electric dipole moment of the neutron, *Phys. Rev. D* **92**, 092003 (2015).
- [23] I. S. Altarev, Y. V. Borisov, N. V. Borovikova, A. B. Brandin, A. I. Egorov, V. F. Ezhov, S. N. Ivanov, V. M. Lobashev, V. A. Nazarenko, V. L. Ryabov *et al.*, A new upper limit on the electric dipole moment of the neutron, *Phys. Lett. B* **102**, 13 (1981).
- [24] C. Abel, S. Afach, N. J. Ayres, C. A. Baker, G. Ban, G. Bison, K. Bodek, V. Bondar, M. Burghoff, E. Chanel *et al.*, Measurement of the permanent electric dipole moment of the neutron, *Phys. Rev. Lett.* **124**, 081803 (2020).
- [25] C. Abel, N. J. Ayres, G. Ban, G. Bison, K. Bodek, V. Bondar, M. Daum, M. Fairbairn, V. V. Flambaum, P. Geltenbort *et al.*, Search for axionlike dark matter through nuclear spin precession in electric and magnetic fields, *Phys. Rev. X* **7**, 041034 (2017).
- [26] Z. Wang, X. Peng, R. Zhang, H. Luo, J. Li, Z. Xiong, S. Wang, and H. Guo, Single-species atomic comagnetometer based on ^{87}Rb atoms, *Phys. Rev. Lett.* **124**, 193002 (2020).
- [27] N. J. Ayres, G. Bison, K. Bodek, V. Bondar, T. Bouillaud, E. Chanel, P.-J. Chiu, B. Clement, C. B. Crawford, M. Daum *et al.*, Search for an interaction mediated by axion-like particles with ultracold neutrons at the PSI, *New J. Phys.* **25**, 103012 (2023).
- [28] F. Rathmann, N. N. Nikolaev, and J. Slim, Spin dynamics investigations for the electric dipole moment experiment, *Phys. Rev. Accel. Beams* **23**, 024601 (2020).
- [29] D. Eversmann *et al.* (JEDI Collaboration), New method for a continuous determination of the spin tune in storage rings and implications for precision experiments, *Phys. Rev. Lett.* **115**, 094801 (2015).
- [30] Z. Bagdasarian, S. Bertelli, D. Chiladze, G. Ciullo, J. Dietrich, S. Dymov, D. Eversmann, G. Fanourakis, M. Gaisser, R. Gebel *et al.*, Measuring the polarization of a rapidly precessing deuteron beam, *Phys. Rev. ST Accel. Beams* **17**, 052803 (2014).
- [31] Jülich Electric Dipole moment Investigations <http://collaborations.fz-juelich.de/ikp/jedi/>.
- [32] N. Hempelmann *et al.* (JEDI Collaboration), Phase locking the spin precession in a storage ring, *Phys. Rev. Lett.* **119**, 014801 (2017).
- [33] N. N. Nikolaev *et al.* (JEDI Collaboration), Spin decoherence and off-resonance behavior of radio-frequency-driven spin

- rotations in storage rings, *Phys. Rev. Accel. Beams* **27**, 111002 (2024).
- [34] J. Slim *et al.* (JEDI Collaboration), First detection of collective oscillations of a stored deuteron beam with an amplitude close to the quantum limit, *Phys. Rev. Accel. Beams* **24**, 124601 (2021).
- [35] J. Slim, R. Gebel, D. Heberling, F. Hinder, D. Hölscher, A. Lehrach, B. Lorentz, S. Mey, A. Nass, F. Rathmann *et al.*, Electromagnetic simulation and design of a novel waveguide rf Wien filter for electric dipole moment measurements of protons and deuterons, *Nucl. Instrum. Methods Phys. Res. Sect. A* **828**, 116 (2016).
- [36] J. Slim, A. Nass, F. Rathmann, H. Soltner, G. Tagliente, and D. Heberling, The driving circuit of the waveguide rf Wien filter for the deuteron EDM precursor experiment at COSY, *J. Inst.* **15**, P03021 (2020).
- [37] V. Hejny, A. Andres, J. Pretz, F. Abusaif, A. Aggarwal, A. Aksentev, B. Alberdi, L. Barion, I. Bekman, M. Beyß *et al.* (JEDI Collaboration), Maintaining a resonance condition of an rf spin rotator through a feedback loop in a storage ring, *Phys. Rev. Accel. Beams* **28**, 062801 (2025).
- [38] V. D. Kekelidze, R. Lednicky, V. A. Matveev, I. N. Meshkov, A. S. Sorin, and G. V. Trubnikov, Three stages of the NICA accelerator complex, *Eur. Phys. J. A* **52**, 211 (2016).
- [39] M. Froissart and R. Stora, Depolarisation d'un faisceau de protons polarises dans un synchrotron, *Nucl. Instrum. Methods* **7**, 297 (1960).
- [40] NIST database, <http://physics.nist.gov/cuu/Constants/index.html>.
- [41] A. Saleev *et al.* (JEDI Collaboration), Spin tune mapping as a novel tool to probe the spin dynamics in storage rings, *Phys. Rev. Accel. Beams* **20**, 072801 (2017).
- [42] F. Müller, O. Javakhishvili, D. Shergelashvili, I. Keshelashvili, D. Mchedlishvili, F. Abusaif, A. Aggarwal, L. Barion, S. Basile, J. Böker *et al.*, A new beam polarimeter at COSY to search for electric dipole moments of charged particles, *J. Instrum.* **15**, P12005 (2020).
- [43] Barthel HF-Technik GmbH, 52072 Aachen, Germany <https://barthel-hf.com>
- [44] Model SMB100A, Rohde & Schwarz GmbH & Co. KG, Munich, Germany, <http://www.rohde-schwarz.de>
- [45] F. Bloch, Nuclear induction, *Phys. Rev.* **70**, 460 (1946).
- [46] I. Nakagawa *et al.*, RHIC polarimetry, *Eur. Phys. J. Spec. Top.* **162**, 259 (2008).
- [47] W. Fischer and A. Bazilevsky, Impact of three-dimensional polarization profiles on spin-dependent measurements in colliding beam experiments, *Phys. Rev. ST Accel. Beams* **15**, 041001 (2012).
- [48] H. Huang, J. Kewisch, C. Liu, A. Marusic, W. Meng, F. Méot, P. Oddo, V. Ptitsyn, V. Ranjbar, and T. Roser, High spin-flip efficiency at 255 GeV for polarized protons in a ring with two full Siberian snakes, *Phys. Rev. Lett.* **120**, 264804 (2018).
- [49] H. Huang, J. Kewisch, C. Liu, A. Marusic, W. Meng, F. Méot, P. Oddo, V. Ptitsyn, V. Ranjbar, T. Roser *et al.*, Measurement of the spin tune using the coherent spin motion of polarized protons in a storage ring, *Phys. Rev. Lett.* **122**, 204803 (2019).
- [50] R. G. Carter, Radio-frequency power generation, CERN Yellow Report CERN-2013-001, CERN Document Server (CERN, Geneva, 2013), doi:10.5170/CERN-2013-001.45.
- [51] S. Karanth *et al.* (JEDI Collaboration), First search for axionlike particles in a storage ring using a polarized deuteron beam, *Phys. Rev. X* **13**, 031004 (2023).